Calorimetric study of nematic–smectic-A tricritical behavior in mixtures of heptyloxypentylphenylthiolbenzoate and octyloxycyanobiphenyl

M. E. Huster,* K. J. Stine, and C. W. Garland
Department of Chemistry and Center for Material Science and Engineering, Massachusetts Institute of Technology, Cambridge, Massachusetts 02139
(Received 23 March 1987)

The critical heat capacity associated with the nematic (N) to smectic-A (SmA) phase transition has been studied in mixtures of nonpolar heptyloxypentylphenylthiolbenzoate ($\overline{7}$S5) and polar octyloxycyanobiphenyl (8OCB). In this system, which exhibits both an N-SmA-SmC multicritical point and an N-SmA tricritical point, the N-SmA transition temperature T_{NA} increases very rapidly as the 8OCB mole fraction X is increased. Data were obtained for a sample near the tricritical composition, for two compositions where the N-SmA transition is second order, and for three compositions exhibiting weakly-first-order transitions. Because of the large values of dT_{NA}/dX, Fisher renormalization was observed. The finite cusp in C_p near the tricritical point yields the renormalized critical exponent $\alpha_R = -0.93 \pm 0.17$. Since $\alpha_R = -\alpha/(1-\alpha)$, this corresponds to $\alpha = 0.48 \pm 0.05$, in good agreement with the value 0.5 expected at a Gaussian tricritical point.

I. INTRODUCTION

Mixtures of the nonpolar liquid crystal heptyloxypentylphenylthiolbenzoate ($\overline{7}$S5) and the polar liquid crystal octyloxycyanobiphenyl (8OCB) exhibit an interesting phase diagram in the $\overline{7}$S5-rich region. Pure $\overline{7}$S5 undergoes a nematic (N) to smectic-C (SmC) transition. Addition of a small amount of 8OCB gives rise to a nematic–smectic-A–smectic-C (NAC) multicritical point at 8OCB mole fraction $X_{NAC} = 0.0217$ (wt % 8OCB = 1.68) and $T_{NAC} = 314.95 \pm 0.2$ K.[1,2] The phase boundaries in the NAC multicritical region conform well with the universal NAC phase-diagram topology established in mixtures by Brisbin *et al.*[3] and confirmed by Shahidhar *et al.*[4] in pressure studies of pure compounds. As the 8OCB content is further increased, the nematic–smectic-A (SmA) transition temperature T_{NA} increases rapidly from the NAC point to a nematic–smectic-A–isotropic (I) triple point at $X_{8OCB} \simeq 0.35$ and $T_{NAI} \simeq 372$ K.

Recent investigations of $\overline{7}$S5 + 8OCB mixtures[1,2,5,6] have focused on multicritical NAC behavior, which has been extensively but somewhat inconclusively studied in other systems for a decade (see references cited in Ref. 2). Light scattering[5] and x-ray scattering[1,2] results on $\overline{7}$S5 + 8OCB show that the NAC behavior in the system is best described by a Lifshitz-point model.[7] Neither x-ray nor heat-capacity[6] investigations of the N-SmC transition region near the NAC point show evidence of a biaxial nematic phase that should exist if the NAC point is a decoupled tetracritical point.[8]

We have carried out a high-resolution ac calorimetric study of the $C_p(T)$ variation associated with the N-SmA transition as a function of 8OCB concentration. The N-SmA heat capacity has not been studie very close to the NAC point since the correlation lengths for SmA fluctuations grow rapidly as $X \rightarrow X_{NAC}$,[2,5] which leads to very small C_p peaks due to two-scale-factor universality.[9–11] The results reported here are for samples ranging from $X = 0.0326$ (2.53 wt. % 8OCB) to $X = 0.1012$ (7.99 wt. % 8OCB). The phase diagram for $X \leq 0.125$, shown in Fig. 1, is based on the present work and results reported in Refs. 2 and 12. The investigated composition range contains a N-SmA tricritical point that is estimated to be at $X_t \simeq 0.063$ and $T_t \simeq 337.3$ K. An almost tricritical sample with $X = 0.0614$, two second-order samples, and two samples undergoing a weakly-first-order transition have been studied in detail. The tricritical N-SmA behavior in this mixture of unlike molecules (one polar and one nonpolar) will be compared to that reported for mixtures of like mol-

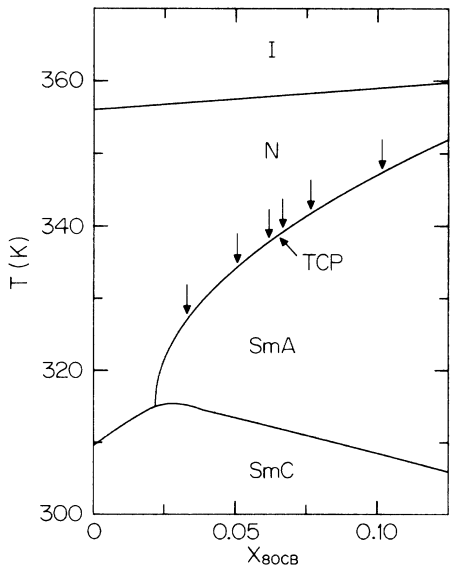

FIG. 1. Partial phase diagram for $\overline{7}$S5 + 8OCB liquid-crystal mixtures; X_{8OCB} is the mole fraction of 8OCB. The compositions of the samples studied are indicated by the small vertical arrows, and the estimated position of the N-SmA tricritical point is also indicated.

ecules (members of a homologous series).[12–16] In contrast to other systems, the $\overline{7}$S5 + 8OCB tricritical point occurs when the N-I and N-SmA transitions are still quite far apart ($T_{NI}-T_{NA}=20.7$ K or a McMillan ratio $T_{NA}/T_{NI}=0.942$). Furthermore, the slope of the T_{NA} transition line $dT_{NA}/dX=289$ K at the tricritical point is much larger than that observed in other systems.

As a result of the steep phase boundary, Fisher renormalization of the critical exponents[17] is observed. The effect of Fisher renormalization on the heat capacity is quite significant since a power-law divergence (critical exponent $\alpha>0$) becomes a finite cusp ($\alpha_R<0$). Second-order N-SmA transitions are often characterized by effective heat-capacity exponents as large as $\alpha\simeq 0.2$ to 0.3 (Ref. 18) and the tricritical exponent is 0.5; thus Fisher renormalization makes a dramatic change in the shape of the $C_p(T)$ peak. These $\overline{7}$S5 + 8OCB mixtures represent what we believe to be the best established example of Fisher renormalization near a tricritical point. The underlying (unrenormalized) values of α are consistent with the crossover behavior from second order to tricritical seen in homologous liquid-crystal mixtures.[12,14,16] However, the overall tricritical N-SmA behavior in liquid crystals does not conform exactly to Gaussian tricritical predictions and remains a challenging theoretical problem.

II. METHOD AND RESULTS

The ac calorimeter used in this work is a microcomputer-controlled automated instrument that has been described in detail elsewhere.[19] The essential features will be reviewed briefly. A silver sample cell containing ~ 0.1 g of liquid crystal is hermetically sealed with a cold-welded indium seal. The system operates at a constant frequency $\omega=0.196$ (i.e., 32 sec period), and the sample undergoes zero-to-peak temperature oscillation of about 6 mK for a power input of 0.5 mW. The temperature of the thermostat bath can be scanned slowly up or down. The typical scan rate for data taken near the transition is 70 mK/h within ± 0.5 K of T_c and 360 mK/h in the range $0.5\ \text{K} < |T-T_c| < 2.5$ K, while faster scans of ~ 1.3 K/h were used over a broad temperature range to provide the overall background variation in C_p. For the almost-tricritical ($X=0.0614$) sample even slower scans were used close to T_c: 26 mK/h for $|\Delta T|<0.3$ and 60 mK/h for $0.3\ \text{K} < |\Delta T| < 0.7$ K.

The ac technique has been used as an absolute method to determine the specific heat $\bar{C}_p$ (heat capacity per gram of sample),

$$\bar{C}_p=\frac{C_p(\text{obs})-C_p(\text{empty})}{m}\ , \tag{1}$$

where C_p(obs) represents the total heat capacity of the filled cell, C_p(empty) denotes the heat capacity of the empty cell, and m is the mass of the liquid-crystal mixture in grams. The value of C_p(empty) was calculated from the known weights and measured specific heats of all the components used to construct the cell. There may be small systematic errors in the absolute values of $\bar{C}_p$ due to imperfect correction for the heat leak through the electrical leads, possible nonuniform heat flux over the area of the cell, and any errors in the assessment of C_p(empty). However, such errors are not important for the present purpose of determining the temperature dependence of $\bar{C}_p$ near the N-SmA transition. Absolute temperature values were obtained by calibrating the thermistor attached to the cell with a platinum resistance thermometer mounted in a metal block attached to the sample holder. The resulting thermistor temperatures are estimated to have an absolute accurate of ± 50 mK, but this is not a limiting factor since we are concerned with analyzing the dependence of $\bar{C}_p$ on the temperature difference $T-T_c$.

The structural formulas for 8OCB and $\overline{7}$S5 are given below:

8OCB: $C_8H_{17}O$–⟨⟩–⟨⟩–CN

$\overline{7}$S5: $C_7H_{15}O$–⟨⟩–COS–⟨⟩–C_5H_{11} .

The 8OCB was obtained from the British Drug House; a 99.8%-purity sample of $\overline{7}$S5 was obtained from the Liquid Crystal Institute at Kent State University. The materials used in the calorimetry were identical to those used for x-ray and light scattering studies.[2,5]

Six samples were studied over a wide temperature range spanning the N-I and N-SmA transitions. The compositions and transition temperature are listed in Table I. In addition, the N-SmC transition near the NAC point was studied previously in a sample with $X=0.01945$ (1.506 wt. % 8OCB).[6] The overall temperature range studied for the samples listed in Table I was from ~ 365 K down to ~ 325 K except for the 0.0326 sample, which was studied down to 310 K (below the monotropic SmA-SmC transition temperature).

The overall variation in $\bar{C}_p$ through both the N-I and N-SmA transitions is shown in Fig. 2 for the 0.0614 sample. Aside from small shifts in temperature, the N-I specific heat peaks are almost identical for all the samples

TABLE I. Compositions of investigated $\overline{7}$S5 + 8OCB samples (in weight percent 8OCB and mole fraction X of 8OCB), the N-I and N-SmA transition temperatures, and the integrated area δH_{NA} of the excess heat capacity associated with the N-SmA transition. The molecular weight is 398.61 g for $\overline{7}$S5 and 307.44 g for 8OCB.

wt. % 8OCB	X	T_{NI} (K)	T_{NA} (K)	δH_{NA} (J g^{-1})
2.53	0.0326	357.2	326.295	1.85
3.93	0.0504	357.6	334.241	2.00
4.80	0.0614	357.8	337.118	2.05
5.20	0.0664	358	337.637	~2.14
5.97	0.0761	358.9	341.6	
7.99	0.1012	359.6	348	

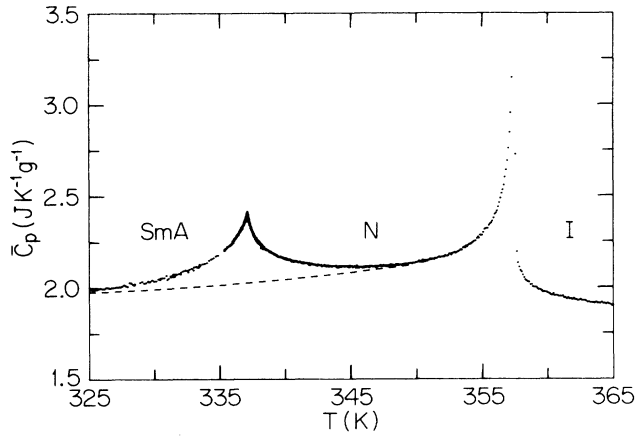

FIG. 2. Specific heat $\bar{C}_p$ for a $\overline{7}$S5 + 8OCB mixture with $X=0.0614$ (4.80 wt. % 8OCB). This mixture is very close to the tricritical composition. The dashed line represents an extension of the N-I heat-capacity peak and defines the quantity $\bar{C}_p(NI)$ used in Eq. (2) to determine $\Delta\bar{C}_p$, the excess specific heat associated with the N-SmA transition.

studied. Figure 3 shows a comparison of the N-I region for the 0.0326 and the 0.0614 samples. This invariance of the N-I peak shape makes it easier to choose a low-temperature "tail" associated with the N-I peak, $\bar{C}_p(NI)$, which serves as a background for determining the excess specific heat in the N-SmA transition region. That is, $\bar{C}_p(NI)$ represents the specific-heat variation that would occur if *only* the N-I transition took place. The $\bar{C}_p(NI)$ curve chosen for the 0.0614 sample is shown by the dashed line in Fig. 2.

Slow scans carried out in the region of T_{NA} provide a dense data set for later analysis. The excess specific heat $\Delta\bar{C}_p$ associated with the N-SmA transition is obtained from

$$\Delta\bar{C}_p=\bar{C}_p-\bar{C}_p(NI)\ . \tag{2}$$

Figure 4 shows the $\Delta\bar{C}_p$ variation for the 0.0614 sample.

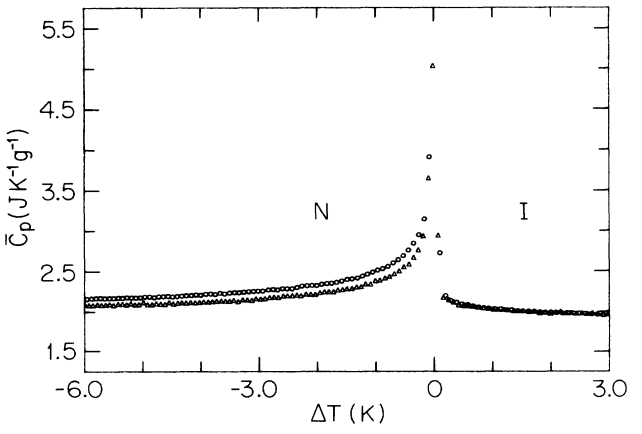

FIG. 3. Comparison of the N-I specific-heat peaks for samples with $X=0.0326$ (Δ) and $X=0.0614$ (○); $\Delta T\equiv T-T_{NI}$. The $\bar{C}_p$ values for the 0.0326 sample have been shifted down by 0.50 to facilitate comparison.

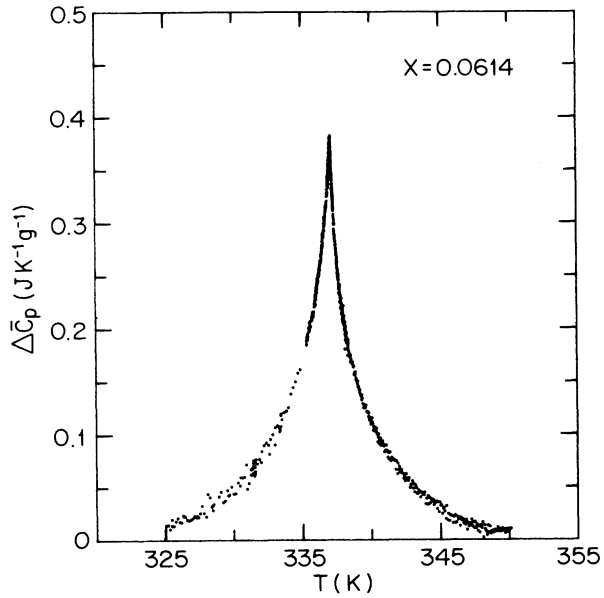

FIG. 4. Excess specific heat $\Delta\bar{C}_p$ associated with the N-SmA transition in the nearly tricritical $\overline{7}$S5 + 8OCB sample with $X=0.0614$.

The $\Delta\bar{C}_p$ variations for the other five samples are shown in Fig. 5. The 0.0614 data are shown separately for two reasons: (a) this sample is very close to the tricritical composition, as discussed below, and (b) the 0.0614 data points lie sufficiently close to those for the 0.0664 sample that confusion arises if both data sets are included in Fig.

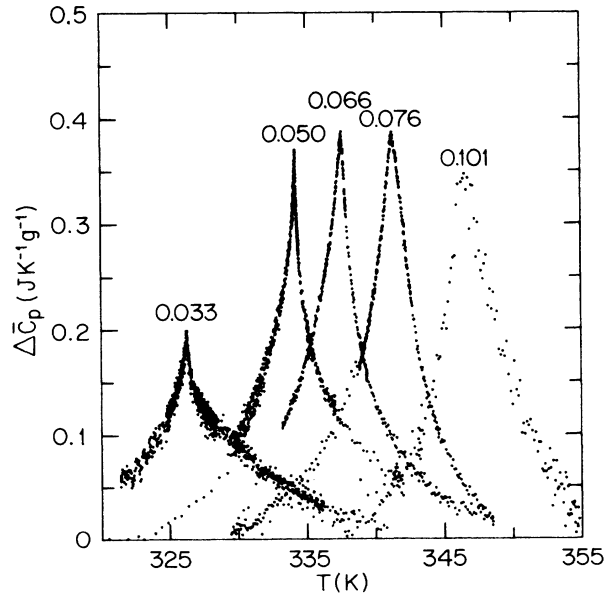

FIG. 5. Excess specific heats $\Delta\bar{C}_p$ associated with second-order N-SmA transitions ($X=0.0326$ and 0.0504), a very weakly first-order N-SmA transition that is close to the tricritical point ($X=0.0664$), and definitely first-order transitions (0.0761 and 0.1012). The data on the 0.1012 sample represent a rapid survey scan intended merely to sketch the position and size of this peak.

5. Note that the sparse data for the 0.1012 sample represent a rapid survey run to determine the rough size and shape of $\Delta\bar{C}_p$ for this first-order N-SmA transition.

It is obvious from Figs. 4 and 5 that all these N-SmA specific heat runs exhibit nondivergent peaks which are broad compared to typical N-SmA peaks reported previously.[11,12] The integrated enthalpy changes

$$\delta H_{NA} = \int \Delta\bar{C}_p dT \ , \tag{3}$$

listed in Table I, are also large compared to those in usual second-order N-SmA transitions (0.2–2.0 J g^{-1}).[12,20]

For a better display of the detailed behavior near T_{NA}, Fig. 6 shows $\Delta\bar{C}_p$ versus $\Delta T = T - T_{NA}$ on two expanded scales: ± 1.5 K and ± 0.15 K. These plots show clearly that the N-SmA heat-capacity peaks exhibit finite cusps. Several runs made on the 0.0326, 0.0504, and 0.0614 samples showed no hysteresis and no indications of rounding or truncation near the top of the peak. For the 0.0664 sample, a distinct rounding of the $\Delta\bar{C}_p$ peak occurs over a 0.39-K interval marked by the small arrows in Fig. 6. The data for the 0.0761 sample exhibit a marked distortion near the transition and distinct hysteresis. Figure 7 shows some of the $\Delta\bar{C}_p$ data obtained on warming and cooling runs for this sample. The heating and cooling data agree very well over a wide range (not shown in Fig. 7) but clearly disagree over a 1.34-K interval close to the transition.

We consider that both the 0.0664 and 0.761 samples undergo weakly-first-order N-SmA transitions,[21] whereas there is no indication of first-order character for the 0.0614 sample. Thus the tricritical mole fraction x_{NAC} is 0.0614 or some value between 0.0614 and 0.0664. Since the distortion of the 0.0664 peak is limited to a 390-mK region, those data points were omitted and the remaining data were analyzed in terms of the same theoretical expression used to fit the 0.0614 data. The size and shape of the $\Delta\bar{C}_p$ peaks for the 0.0614 and 0.0664 samples are very similar, and the resulting fit parameters agree quite well, as shown in Sec. III. Thus it was not felt necessary to study another sample with an intermediate composition around $x = 0.063$. No attempts were made to carry out a theoretical analysis of the data from the 0.0761 or 0.1012 samples.

III. DATA ANALYSIS

Let us begin with a brief description of the theoretical form to be used in fitting the N-SmA data shown in Fig. 6. For many pure liquid-crystal compounds and binary mixtures of homologous compounds, the excess heat capacity associated with fluctuations near a N-SmA second-order transition can be represented by a simple power law

$$\Delta C_p = A_1 t^{-\alpha} + B_1 \tag{4}$$

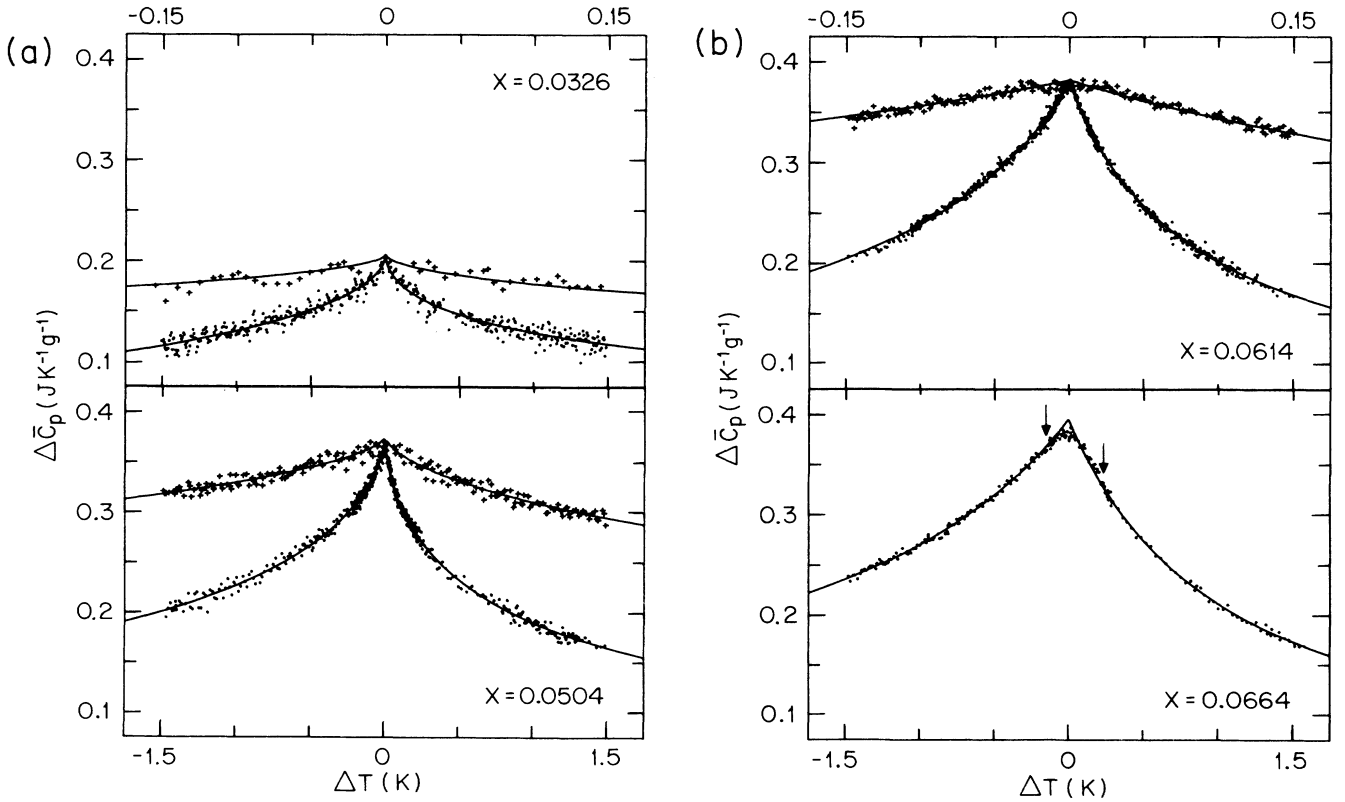

FIG. 6. Detailed views of $\Delta\bar{C}_p$ on two expanded scales $\Delta T = T - T_{NA} = \pm 1.5$ K (lower data set ●) and ± 0.15 K (upper data set +). The smooth curves represent fits with Eq. (9) as described in Sec. III. For the sample with $X = 0.0664$, the peak is rounded and all data between the two small arrows were omitted from the fitting procedure; see text for further details.

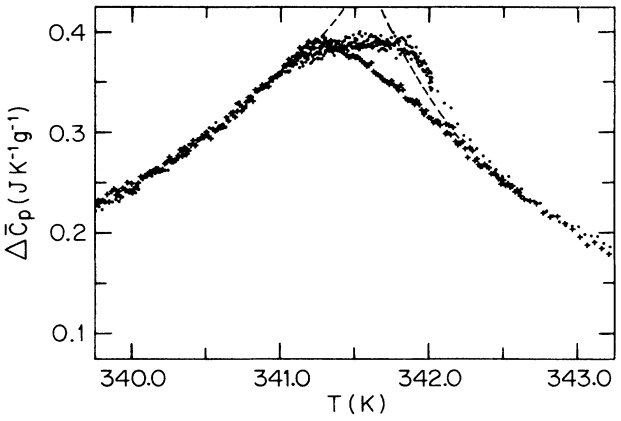

FIG. 7. Detailed view of the hysteresis observed very close to the N-SmA transition in a $\overline{7}$S5 + 8OCB sample with $X=0.0761$. Data on warming (+) and cooling (●) runs agree very well over a range of several degrees above and below the range shown here. The dashed curve represents the variation expected if this transition had been continuous rather than first order with a coexistence range and hysteresis.

or a form including a corrections-to-scaling term

$$\Delta C_p = A_1 t^{-\alpha}(1+D_1 t^{0.5})+B_1 , \tag{5}$$

where $t = |(T-T_c)/T_c|$ is the reduced temperature. In most cases α is positive, which implies that ΔC_p diverges at T_c.[11–14] For mixtures, one should in principle measure $\Delta C_{p\phi}$ as a function of t_ϕ, where constant ϕ designates a path of constant chemical potential difference. For mixtures of liquid-crystal homologs, the distinction between C_{pX} and $C_{p\phi}$ does not seem to be important (probably due to the small values of dT_c/dX, see Ref. 22) and no apparent problems arise in analyzing the data with Eqs. (4) or (5).[13–16]

In the present system, however, the distinction between constant mole fraction X and constant chemical potential difference ϕ is important. Our experiments, carried out at constant composition, yield values of ΔC_{pX} as a function of the reduced temperature t_X. Fisher[17] has shown that t_ϕ and t_X are related by

$$t_\phi(1+\varepsilon')+\varepsilon t_\phi^{1-\alpha}=t_X(1+\varepsilon'') , \tag{6}$$

where $\varepsilon \sim (dT_c/dX)^2$ is a measure of the magnitude of the deviation from ideal behavior, and ε' and ε'' are both small quantities proportional to ε. If $\varepsilon \ll 1$, then $t_\phi \sim t_X$ and $\Delta C_{p\phi} \sim \Delta C_{pX}$, which means that no "Fisher renormalization" occurs. If ε is sufficiently large, there will be a physically accessible region close to T_c where $t_\phi^{1-\alpha} \sim t_X$ since $t_\phi^{1-\alpha}$ goes to zero slower than t_ϕ. In this region one finds[23]

$$\Delta C_{pX} = B - \frac{A t_X^{-\alpha_R}}{1+D t_X^{-\alpha_R}} , \tag{7}$$

where the renormalized heat-capacity exponent $\alpha_R < 0$ is defined by

$$\alpha_R \equiv -\alpha/(1-\alpha) . \tag{8}$$

The size of the reduced temperature region over which Eq. (7) is valid depends on the magnitude of dT_c/dX and α.[17,22] Large values of $(dT_c/dX)^2$ and large positive values of α imply a large region of Fisher renormalization. We have already noted that dT_{NA}/dX is large for the $\overline{7}$S5 + 8OCB system. Furthermore, the effective exponent α is quite large (>0.2) for many second-order N-SmA transitions[11,12] and is ~ 0.5 at several N-SmA tricritical points.[12–16] Thus Fisher renormalization should occur over a wider reduced temperature range than that predicted[17] and seen[24] for Ising systems.

We will show below that excellent fits to $\Delta\bar{C}_p$ can be obtained with the fully renormalized form (7) in which the scaling relations $\alpha_R^+ = \alpha_R^- = \alpha_R$ and $B^+ = B^- = B$ are imposed. Thus we will use the form

$$\Delta\bar{C}_p^{\pm} = B - \frac{A^{\pm} t^{-\alpha_R}}{1+D^{\pm} t^{-\alpha_R}} , \tag{9}$$

where the superscript denotes above (+) or below (−) T_c and t is, of course, the experimentally accessible t_X. In order to test the compatibility of the data to the scaling equalities for α and B, we also carried out independent fits to the SmA data alone and the N data alone. Details will not be given, but scaling was well obeyed in all cases. Typical results were $\Delta\alpha_R/\alpha_R = |\alpha_R^+ - \alpha_R^-|/\alpha_R = 0.05$ and $\Delta B/B = |B^+ - B^-|/B = 0.01$.

In fitting the $\Delta\bar{C}_p$ data, there are six adjustable parameters $\alpha_R, B, A^+, D^+, A^-$, and D^- since T_c is taken to be the temperature where $\Delta\bar{C}_p$ exhibits its maximum. Allowing T_c to be another free parameter typically alters this value by less than ± 1 mK and does not change the other fit parameters significantly. The least-squares parameters for fits with Eq. (9) over the range $|T-T_c| \leq 1.5$ K ($t < 4.5\times 10^{-3}$) are given in Table II. These parameters are quite stable when the range is expanded to $|\Delta T| \leq 3.5$ K or shrunk to $|\Delta T| \leq 0.15$ K.[25] The standard deviation in the critical exponent α_R obtained from the least-squares-fitting routine is given in Table II. Note that the uncertainty figure is quite large for the 0.0326 sample. This is due partly to the small magnitude of this excess heat capacity and partly to a small but systematic oscillation in the 0.0326 data points (see Fig. 6). The latter was caused by imperfect bath-temperature regulation during the 0.0326 run and is also reflected in the larger χ_ν^2 value.

The 95% confidence limits on each α_R value were obtained by stepping α through the region of its minimum and applying the F test. For the 0.0614 sample, the variation of χ_ν^2 with α_R is shown in Fig. 8 and one obtains $\alpha_R = -0.925 \pm 0.17$. For the other samples, the results are $\alpha_R = -0.99 \pm 0.43$ ($X=0.0664$) and $\alpha_R = -0.65 \pm 0.26$ ($X=0.0504$). In the case of the 0.0326 sample, the χ_ν^2 minimum is very broad and the F test does not provide physically reasonable limiting fits. We estimate that $\alpha_R = -0.55^{+0.25}_{-0.40}$ ($X=0.0326$).

The quality of the fits is indicated by the smooth curves shown in Fig. 6 as well as the χ_ν^2 values. It should be not-

TABLE II. Least-squares fitting parameters obtained from a simultaneous fit of data in the N and SmA phases with Eq. (9). The units of $A^{\pm}$ and B are J K^{-1} g^{-1}; $t_{\min}$ denotes the smallest value of reduced temperature used in fits above (+) and below (−) T_c. The number of degrees of freedom $\nu = N - 6$, where N is the number of data points. The uncertainties for the α_R values are the standard deviations given by the fitting routine; T_c values are fixed at the values given in parentheses.

X 8OCB	T_c (K)	$t_{\min}$	α_R	B	A^+	A^-/A^+	D^+	D^-/D^+	ν	χ^2_ν
0.0326	(326.295)	-5.5×10^{-5} $+5.8\times10^{-5}$	−0.551±0.17	0.2066	2.962	0.7607	13.72	0.3843	425	1.64
0.0504	(324.241)	-1.5×10^{-5} $+1.8\times10^{-5}$	−0.653±0.03	0.3752	15.71	0.6541	40.50	0.6137	492	1.38
0.0614	(337.118)	-1.5×10^{-5} $+1.8\times10^{-5}$	−0.925±0.02	0.3824	80.15	0.6368	224.7	0.6138	683	1.05
0.0664	(337.637)	-4.7×10^{-4} $+6.8\times10^{-4}$	−0.991±0.05	0.3958	113.3	0.5467	295.2	0.5838	179	0.81

ed that there are no systematic trends in the deviations between the data and the theoretical curves except for the 0.0664 data close to the transition. As discussed in Sec. II, the specific-heat peak was systematically rounded in all runs done on the 0.0664 sample. The data points lying between the two arrows in Fig. 6, which were omitted from the fit, clearly show the character of this rounding. Note also that the term $Dt^{-\alpha_R}$ in Eq. (9) is substantial in all the fits and plays a significant role when $t > 3\times10^{-4}$. A fit with the simple form $B - At^{-\alpha_R}$ (i.e., $D^{\pm}=0$) over the range $t \leq 3.5\times10^{-4}$ yields α_R values consistent with those given in Table II. However, such fits are very poor over a wider range and cannot be improved in a self-consistent way by adding an empirical "correction term" to give the form $B - At^{-\alpha_R}(1+D_1 t^{\Delta})$. The latter form can mimic the data over a moderate range but exhibits very large systematic deviations on range expansion.

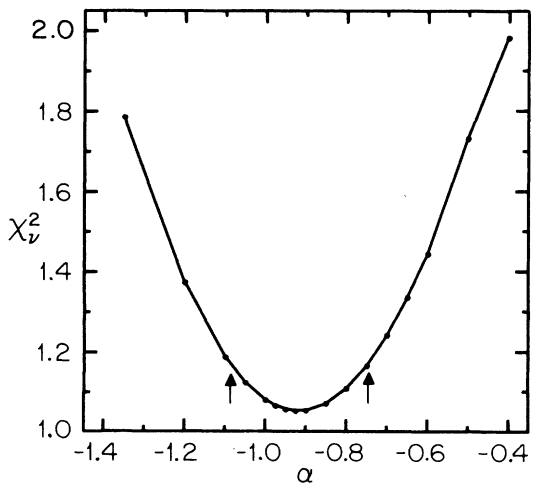

FIG. 8. χ^2_ν values for least-squares fit to $\Delta\bar{C}_p$ on the 0.0614 sample as a function of fixed values of α_R. For this data set, 95% confidence limits correspond to $\chi^2_\nu/\chi^2_\nu(\min) = F(677,677) = 1.13$. These 95% confidence limits are indicated by the two small arrows.

IV. DISCUSSION

The N-SmA phase boundary is steep over the entire range as shown in Fig. 1. Table III shows that the value of (dT_{NA}/dX) at the tricritical point is much larger for $\bar{7}$S5 + 8OCB than for any other liquid-crystal system exhibiting a N-SmA tricritical point. Thus Fisher renormalization, which depends on the magnitude of $(dT_{NA}/dX)^2$, is expected to occur and is seen in all our samples. The only other case of Fisher renormalization in liquid crystals known to us involves the SmA_1-SmA_2 transition in a hexylphenylcyanobenzoyloxybenzoate and terephtal-bisbutyl aniline mixture (DB$_6$+TBBA).[26–28] In this case $(dT_c/dX) \simeq 163$ K and Fisher-renormalized Ising exponents were observed. Both the $\bar{7}$S5 + 8OCB and DB$_6$+TBBA systems involve mixtures of one polar and one nonpolar component. It seems physically reasonable that constant-X and constant-ϕ paths would not be equivalent in a binary mixture of such dissimilar molecules. No indications of Fisher renormalization are observed in mixtures of two polar homologs (8CB + 10CB) (Ref. 16) or two nonpolar homologs ($60\bar{1}0+60\bar{1}2$),[13] (40.8+60.8).[14]

Assuming that the critical exponents found from fitting our data with Eq. (9) are fully Fisher renormalized, we can obtain the underlying exponents α from Eq. (8). In the case of the tricritical region, the 0.0614 sample yields $\alpha = 0.48\pm0.05$, which is confirmed by the somewhat less reliable value obtained from the 0.0664 sample ($\alpha = 0.50\pm0.11$). The uncertainties quoted here correspond to 95% confidence limits. The exponent value 0.48 is in good agreement with α_t values for other N-SmA tricritical systems, as shown in Table III. It also agrees well with the theoretical Gaussian tricritical value of $\frac{1}{2}$. However, it should be noted that for 9CB and $\bar{1}0$S5, the only systems in which tricritical behavior has been studied with x rays, the correlation exponents $\nu_\parallel$ and $\nu_\perp$ and the susceptibility exponent γ do not quite agree with the Gaussian tricritical exponents $\nu_\parallel = \nu_\perp = \frac{1}{2}$ and $\gamma = 1$. For 9CB $\nu_\parallel = 0.57\pm0.03$, $\nu_\perp = 0.37\pm0.05$, $\gamma = 1.09\pm0.05$, while for $\bar{1}0$S5 $\nu_\parallel = 0.61\pm0.03$, $\nu_\perp = 0.51\pm0.05$, $\gamma = 1.10\pm0.05$.[29] Table III also shows that the heat-capacity amplitude ratios A^-/A^+ do not exhibit a universal value, and the

TABLE III. Comparison of several liquid-crystal systems near their N-SmA tricritical points (TCP's). $\Delta T = T_{NI} - T_{NA}$ is the width of the nematic range at the tricritical composition.

System	Ref.	T_{NI}	T_{NA}	ΔT	T_{NA}/T_{NI}	dT_{NA}/dX	α_t	A^-/A^+
$\overline{10}$S5 (near TCP)	12	358.56	352.45	6.11	0.983	~ -5.53	0.45 ± 0.05	~ 1.7
$\overline{60}\overline{10} + 60\overline{12}$ ($X_{12} = 0.40$)	13	361.86	359.03	2.83	0.992	5.31	0.52	1.38
40.8 + 60.8 ($X_6 = 0.35$)	14	353.42	345.76	7.66	0.978	19.28	0.51 ± 0.06	1.47
9CB + 1OCB ($X_{10} \simeq 0$)	15	322.75	320.85	1.90	0.994	5.30	0.50 ± 0.05	1.00 ± 0.05
8CB + 1OCB ($X_{10} = 0.3135$)	16	316.96	314.26	2.70	0.991	10.80	0.50 ± 0.02	1.00 ± 0.05
$\overline{7}$S5 + 8OCB ($X_{8OCB} \simeq 0.0614$)		357.8	337.12	20.7	0.942	289	0.48 ± 0.05	(0.64)[a]

[a]This is the ratio for the Fisher-renormalized peak amplitudes obtained from Eq. (9). Since the C_p peak is a finite cusp in this case, any ratio $A^-/A^+ < 1$ means that the excess heat capacity below T_c is *larger* than that above T_c.

liquid-crystal values clearly disagree with the ^{3}He-^{4}He tricritical value of ~ 7.[30] This nonuniversality in amplitude ratios indicates that measurements have not been made sufficiently close to the tricritical point to obtain universal behavior.[31] It seems likely that nonuniversal, nonasymptotic amplitude ratios can be reasonably well described in terms of a single parameter $z \sim (a/R_0)^3$, where R_0 defines the range of interactions relative to a microscopic length a.[32] Qualitatively, the liquid-crystal tricritical region is characterized by a z value larger than that for the ^{3}He-^{4}He tricritical region ($z = 0.12$), which implies that liquid-crystal tricriticality is further away from the classical tricritical behavior obtained at $z = 0$.

For the samples that undergo second-order N-SmA transitions, the unrenormalized α values are 0.35 ± 0.13 for the 0.0326 sample and 0.40 ± 0.11 for the 0.0504 sample. These are similar to the effective second-order exponents observed in other systems that are not too far from a tricritical point; for example, $\alpha = 0.30$ for 8CB.[33]

The N-SmA transition in $\overline{7}$S5 + 8OCB has been studied in the vicinity of the NAC multicritical point with x-ray and light scattering techniques.[2,5] For the analysis of samples in the composition range $X = 0.0219$–0.0260, it was found necessary to take into account the effect of the curvature of the phase boundary on the observed divergences. For samples with $X = 0.0346$ and 0.0356, the curvature of the phase boundary had no effect on the critical exponents; and these samples yield $\nu_\parallel = 0.90 \pm 0.03$, $\nu_\perp = 0.78 \pm 0.04$, and $\gamma = 1.59 \pm 0.06$. We believe that such unusually large exponents represent the Fisher renormalized values $\nu_R = \nu/(1-\alpha)$ and $\gamma_R = \gamma/(1-\alpha)$. Using our value of $\alpha = 0.35$ for this composition range, we obtain the underlying true exponents $\nu_\parallel = 0.58 \pm 0.02$, $\nu_\perp = 0.505 \pm 0.025$, and $\gamma = 1.03 \pm 0.04$.

Table IV provides a comparison of the unrenormalized critical exponents for $X \simeq 0.034$ and the exponents observed in 8CB, a polar liquid crystal in which the N-SmA transition is second order but not too far from a tricritical point at $X_{10CB} = 0.3135$ in a 8CB + 10CB mixture.[16] The correspondence in exponent values is quite good for α and $\nu_\perp$ but less so for $\nu_\parallel$ and γ. It should be noted that the trends reported previously for nonuniversal N-SmA exponents[18] seem to indicate that the variations in α and $\nu_\perp$ are coupled as are the variations in $\nu_\parallel$ and γ. For example, both α and $\nu_\perp$ agree with XY values (-0.007 and 0.67) in 40.7 but $\nu_\parallel$ and γ do not, whereas $\nu_\parallel$ and γ agree reasonably well with XY values (0.67 and 1.32) in 8CB but α and $\nu_\perp$ do not. Any significance of a coupling in

TABLE IV. Critical exponents associated with the second-order N-SmA transition in a $\overline{7}$S5 + 8OCB mixture with $X \simeq 0.034$ and in 8CB. The theoretical XY-model exponents are also given. Anisotropic hyperscaling predicts that $\alpha + \nu_\parallel + 2\nu_\perp = 2$. The uncertainty value for this quantity is based on standard deviations for the three exponents.

Material	α	$\nu_\parallel$	$\nu_\perp$	γ	$\alpha + \nu_\parallel + 2\nu_\perp$
$X \simeq 0.034$ (obs,renormalized)	-0.55	0.90	0.78	1.58	1.91 ± 0.28
$X \simeq 0.034$ (unrenormalized)	0.35	0.58	0.505	1.03	1.94 ± 0.14
8CB (Refs. 32 and 34)	0.31	0.67	0.51	1.26	2.00 ± 0.13
XY model (Ref. 35)	-0.007	0.67	0.67	1.32	2

the critical behavior of C_p and the transverse correlation length $\xi_\perp$ on one hand and the susceptibility σ and the longitudinal correlation length $\xi_\parallel$ on the other hand is not clear.

In summary, we have observed Fisher-renormalized tricritical behavior in the heat capacity of a $\overline{7}S5 + 8OCB$ mixture with $X=0.0614$. The N-SmA tricritical point in this system occurs at a composition where the stability range of the nematic phase is unusually large: $(T_{NI}-T_{NA})=20.3$ K or $T_{NA}/T_{NI}=0.943$. The second-order N-SmA transition is also Fisher renormalized. The underlying true critical exponents α, $\nu_\parallel$, $\nu_\perp$, and γ for a $X\simeq 0.034$ sample are similar to those in pure 8CB but do not agree with the XY model. The occurrence of full Fisher renormalization is related to the unusually large value of $(dT_{NA}/dX)^2$ in this mixture of a polar and a nonpolar compound. We believe that this system constitutes the best-established example of Fisher renormalization of the critical heat capacity seen in any system other than ^{3}He-^{4}He.[36]

ACKNOWLEDGMENTS

We wish to thank A. Aharony, R. Birgeneau, D. L. Johnson, and L. Martinez-Miranda for helpful and stimulating discussions. This work was supported by the National Science Foundation under Grant No. DMR-84-18718.

*Present address: Energy Science Laboratories, Inc., P.O. Box 85608, San Diego, CA 92138.

[1]L. J. Martinez-Miranda, A. R. Kortan, and R. J. Birgeneau, Phys. Rev. Lett. **56**, 2264 (1986).

[2]L. J. Martinez-Miranda, A. R. Kortan, and R. J. Birgeneau, following paper, Phys. Rev. A **36**, 2372 (1987).

[3]D. Brisbin, D. L. Johnson, H. Fellner, and M. E. Neubert, Phys. Rev. Lett. **50**, 178 (1983).

[4]R. Shashidhar, B. R. Katna, and S. Krishna Prasad, Phys. Rev. Lett. **53**, 2141 (1984).

[5]L. Solomon and J. D. Litster, Phys. Rev. Lett. **56**, 2268 (1986).

[6]C. W. Garland and M. E. Huster, Phys. Rev. A **35**, 2365 (1987).

[7]J.-C. Chen and T. C. Lubensky, Phys. Rev. A **14**, 1202 (1976).

[8]G. Grinstein and J. Toner, Phys. Rev. Lett. **51**, 2386 (1983); G. Grinstein, T. C. Lubensky, and J. Toner, Phys. Rev. B **33**, 3306 (1986).

[9]D. Stauffer, M. Ferer, and M. Wortis, Phys. Rev. Lett. **29**, 345 (1972); P. C. Hohenberg, A. Aharony, B. I. Halperin, and E. D. Siggia, Phys. Rev. B **13**, 2986 (1976).

[10]M. Anisimov, V. Voronov, A. Kulkov, and F. Kholmurodov, J. Phys. (Paris) **46**, 2137 (1985).

[11]R. J. Birgeneau, C. W. Garland, G. B. Kasting, and B. M. Ocko, Phys. Rev. A **24**, 2624 (1981).

[12]D. Brisbin, R. DeHoff, T. E. Lockhart, and D. L. Johnson, Phys. Rev. Lett. **43**, 1171 (1979); D. L. Johnson (private communication).

[13]M. A. Anisimov, V. P. Voronov, A. O. Kulkov, V. N. Petrukhov, and F. Kholmurodov, Mol. Cryst. Liq. Cryst. (to be published).

[14]K. J. Stine and C. W. Garland (unpublished).

[15]J. Thoen, H. Marynissen, and W. van Dael, Phys. Rev. Lett. **52**, 204 (1984).

[16]H. Marynissen, J. Thoen, and W. van Dael, Mol. Cryst. Liq. Cryst. **124**, 195 (1985); J. Thoen (private communication).

[17]M. E. Fisher, Phys. Rev. **176**, 257 (1968); M. E. Fisher and P. E. Scesney, Phys. Rev. A **2**, 825 (1970).

[18]C. W. Garland, M. Meichle, B. M. Ocko, A. R. Kortan, C. R. Safinya, J. J. Yu, J. D. Litster, and R. J. Birgeneau, Phys. Rev. A **27**, 3234 (1983).

[19]C. W. Garland, Thermochim. Acta **88**, 127 (1985) and references cited therein.

[20]G. B. Kasting, K. J. Lushington, and C. W. Garland, Phys. Rev. B **22**, 321 (1980); E. Bloemen and C. W. Garland, J. Phys. (Paris) **42**, 1299 (1981).

[21]This is supported in a qualitative way by x-ray studies of a 0.0935 sample that showed a distinct first-order transition and coexistence of N and SmA phases; L. J. Martinez-Miranda (private communication).

[22]M. A. Anisimov, A. V. Voronel, and E. E. Gorodetskii, Zh. Eksp. Teor. Fiz. **60**, 1117 (1971) [Sov. Phys.—JETP **33**, 605 (1971)].

[23]This is obtained by rewriting Eq. (4) in the form $\Delta C_{p\phi}=A_2 t_X^{\alpha_R}+B_1$ and substituting this into the general expression $\Delta C_X=(a\Delta C_\phi+b)/(\Delta C_\phi+d)$ where a, b, and d are slowly varying and can be treated as constants. Simplification of the result yields Eq. (7).

[24]E. Bloemen, J. Thoen, and W. Van Dael, J. Chem. Phys. **75**, 1488 (1981).

[25]When $|\Delta T|_{\max}$ is varied from 3.5 K to 0.15 K, the values of α_R lie in the range -0.55 to -0.57 for $X=0.0326$, -0.62 to 0.66 for $X=0.0504$, and -0.90 to -1.0 for $X=0.0614$ ($\alpha_R=-0.90$ corresponds to a 3.5-K range and $\alpha_R=-1.0$ to the 0.15-K range, but the χ^2_ν minimum is rather broad in the latter case and α_R values of -0.9 and -1.1 give fits of almost equal quality).

[26]K. K. Chan, P. S. Pershan, L. B. Sorensen, and F. Hardouin, Phys. Rev. Lett. **54**, 1694 (1985); Phys. Rev. A **34**, 1420 (1986).

[27]C. W. Garland, C. Chiang, and F. Hardouin, Liq. Cryst. **1**, 81 (1986).

[28]D. A. Huse, Phys. Rev. Lett. **55**, 2228 (1985).

[29]B. M. Ocko, R. J. Birgeneau, J. D. Litster, and M. E. Neubert, Phys. Rev. Lett. **52**, 208 (1984); B. M. Ocko, R. J. Birgeneau, and J. D. Litster, Z. Phys. B **62**, 487 (1986).

[30]S. T. Islander and W. Zimmermann, Jr., Phys. Rev. A **7**, 188 (1973).

[31]M. J. Stephen, J. Phys. C **13**, L83 (1980); (private communication).

[32]M. E. Fisher and S. Sarbach, Phys. Rev. Lett. **41**, 1127 (1978); (private communication).

[33]J. Thoen, H. Marynissen, and W. Van Dael, Phys. Rev. A **26**, 2886 (1982).

[34]D. Davidov, C. R. Safinya, M. Kaplan, S. S. Dana, R. Schaetzing, R. J. Birgeneau, and J. D. Litster, Phys. Rev. B **19**, 1657 (1979).

[35]J. C. LeGuillon and J. Zinn-Justin, Phys. Rev. Lett. **39**, 95 (1977); Phys. Rev. B **21**, 3976 (1980).

[36]F. M. Gasparini and M. R. Moldover, Phys. Rev. B **12**, 93 (1975); T. Takada and T. Watanabe, J. Low Temp. Phys. **41**, 221 (1980).